McNair Scholars Research Journal

Volume 8 Article 7

2015

Computational Analysis of the Stereoselective Synthesis of Substituted Pyrrolidines

Diamond T. Jones
djone128@emich.edu

COMPUTATIONAL ANALYSIS OF THE STEREOSELECTIVE SYNTHESIS OF SUBSTITUTED PYRROLIDINES

Diamond T. Jones
Dr. Maria C. Milletti, Mentor

ABSTRACT

In this work we use computational methods to study the aza-Cope-Mannich tandem reaction of a substituted oxazolidine to form a formyl pyrrolidine. Pyrrolidine structural motifs are found in natural products, pharmaceutical compounds, and chiral catalysts. Often only one stereoisomer of these compounds is active, while the others are inactive or toxic. Our goal is to determine reaction conditions and substrate characteristics that lead to one stereoisomer preferentially over the others. We focus on an oxazolidine starting material with an electron-withdrawing group at the nitrogen center and a bulky substituent at the alpha position. The long-term objective is to delineate the energy profile for the multi-step reaction of this starting material, to form a specific enantiomer of the pyrrolidine product. This will allow us to determine the effect of the electron-withdrawing group and the bulky substituent on the stereoselectivity of the reaction. The results will aid the experimental group of our collaborators in determining appropriate reaction conditions. Results to date indicate that the presence of the electron-withdrawing group at the nitrogen center increases the activation energy of the first step of the reaction. If this is in fact the rate-determining step, poor product stereoselectivity is expected, as stereochemistry is not established in this step.

INTRODUCTION

Pyrrolidines are chemical compounds whose structure incorporates five-member carbon rings that contain a nitrogen heteroatom. The general structure of a pyrrolidine ring is shown in **Figure 1.** The pyrrolidine moiety serves as one of the building blocks of natural products that occur in agricultural and medicinal compounds (1). A few examples of such compounds are shown in **Figure 2.** In addition, pyrrolidines are precursors to pyrrolizidine alkaloids, which have shown activity as anticancer and antiviral agents, as well as being important in plant-insect relationships (2).

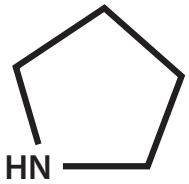

Figure 1. The general structure of an unsubstituted pyrrolidine ring.

There has been extensive research on manipulating pyrrolidines to adapt their properties for pharmaceutical purposes. Results indicate that substituted pyrrolidine derivatives are potential antidepressant agents (3). Pyrrolidines have also been shown to aid in the formation of antitubercular agents. As an example, a series of pyrrolidine derivatives synthesized using a Mannich reaction showed antitubercular activity against Mycobacterium tuberculosis H37Rv. Several other Mannich bases incorporating the pyrrolidine moiety were also found to be active antitubercular agents (4).

In all of these compounds, the stereochemistry of the molecule (the spatial arrangement of atoms) is essential in determining whether the compound is biologically active. Specifically, these compounds contain one or more chiral centers that give rise to two possible spatial arrangements that are mirror images of each other (called *enantiomers*). In practice, one enantiomer is biologically active, while the other is either inactive or sometimes toxic. This is due to the nature of the interaction between the pharmaceutical compound and an enzyme in the biological system: enzymes usually bond with only one enantiomer because of the conformation of their binding site.

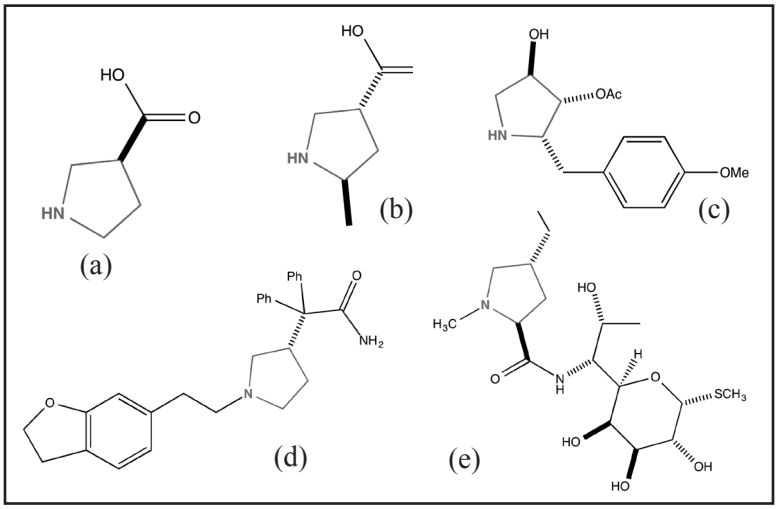

Figure 2. Examples of natural products containing a pyrrolidine moiety: (a) β-Proline, (b) Barbas' catalyst, (c) Anisomycin, (d) Darifenacin, (e) Lincomycin. The pyrrolidine moiety is shown in red.

In addition to the pharmaceutical properties of pyrrolidine-containing compounds, pyrrolidines and their derivatives are widely used as organocatalysts. In other words, they serve as catalysts for organic reactions in which one enantiomer is the target, at the exclusion of the other enantiomer. Again, the spatial arrangement of atoms in the catalyst is important in determining which enantiomer is formed. For example, Barbas has reported the use of β-L-proline and 2-methyl-β-proline (shown in **Figure 2.(a)** and (**b**)) as highly efficient organocatalysts for enantioselective *anti*-Mannich reactions (5). In addition, chiral imizolidinone catalysts have also been shown to provide enantioselectivity in the asymmetric conjugate additions of pyrroles and indoles to enals (6), and in the tandem conjugate reduction-Michael cyclizations of enal enones (7).

The focus of this work is the multi-step reaction of an oxazolidine starting material to form a specific enantiomer of a substituted formyl pyrrolidine (see **Scheme 1.**). An oxazolidine is a five-membered carbon ring that contains two heteroatoms (a nitrogen and an oxygen), as shown in **Figure 3.** The oxazolidine under consideration has two chiral carbon centers (C_3 and C_4 in

Scheme 2.) and can therefore exist as one of four enantiomers, labeled *cis* or *trans,* and *alpha* or *beta.* The labels *alpha* and *beta* refer to whether the formyl group is facing away or toward the observer, respectively. The labels *cis* and *trans* refer to whether the groups at the C_3 and C_4 positions are in the same or opposite orientations, respectively.

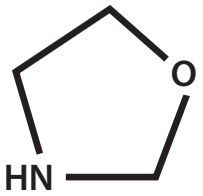

Figure 3. The general structure of an unsubstituted oxazolidine ring.

Here we consider the reaction of the substituted oxazolidine, shown in **Scheme 1.,** with a Lewis acid to produce an iminium cation intermediate. In turn, the iminium cation intermediate can exist as one of eight stereoisomers, labeled *alpha* or *beta,* according to the pyrrolidine enantiomer it leads to, and *boat* or *chair,* according to its conformation. In addition, the iminium cation is labeled *up* if the phenyl substituent is in the same direction as the Lewis acid (BF_3), and labeled *down* if the phenyl substituent is in the opposite direction from the Lewis acid. Each iminium cation undergoes a concerted reaction to form the pyrrolidine product. This is the tandem cationic aza-Cope rearrangement—Mannich cyclization, established and extensively studied by Overman, which is illustrated in **Scheme 1.** (8-11). In this reaction the (3,3) sigmatropic aza-Cope rearrangement is followed by a Mannich cyclization step, to form the pyrrolidine ring.

When the Lewis acid coordinates to the oxygen center of the oxazolidine, the C-O bond is broken, which leads to the formation of one iminium cation stereoisomer. This stereoisomer can follow one of two pathways: aza-Cope – Mannich reaction to the appropriate pyrrolidine product (**Scheme 1**.), or a series of C-C bond rotations that lead to three other iminium cation stereoisomers. The latter pathway is illustrated in **Scheme 2**.

The overarching goal of this project is to model the reactions shown in **Schemes 1**. and **2**., to determine the experimental

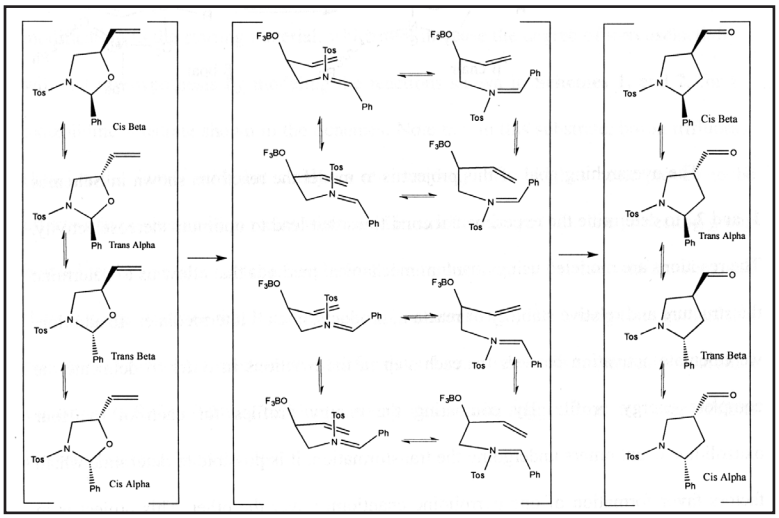

Scheme 1.

conditions that lead to optimum stereoselectivity. The reactions are modeled using quantum mechanical methods that allow us to determine the structure and relative stability of reactant, products, and all intermediates. In addition, we calculate activation barriers for each step in the reactions in order to delineate the complete energy profile. By comparing the energy profiles for each of the four oxazolidine enantiomers undergoing the transformation, it is possible to determine which factors favor formation of one pyrrolidine enantiomer over the other. This project is in collaboration with Prof. Harriet Lindsay in the Chemistry Department at Eastern Michigan University. The Lindsay group is developing a methodology for the stereoselective synthesis of substituted pyrrolidines; as our group models the reaction using a variety of oxazolidine starting materials, we determine the structural characteristics and reaction conditions that optimize stereoselectivity, thus aiding in their methodology development efforts.

My project focuses on determining the effect of adding a bulky substituent at the C_4 position of the oxazolidine starting material. In general, large groups are thought to increase the activation barrier to C-C bond rotations that lead to the scrambling

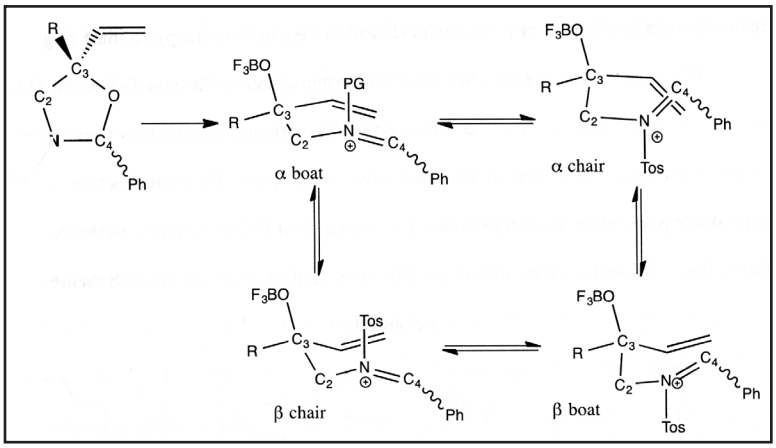

Scheme 2.

of stereoselectivity (cf. **Scheme 2.**) and influence the relative stability of iminium cation stereoisomers. Both of these factors would improve the degree of stereoselectivity. My hypothesis is that adding a phenyl (Ph) substituent at the C_4 position is an advantageous modification to the starting material, which will increase the degree of stereoselectivity. I will test my hypothesis by modeling the reactions shown in **Schemes 1.** and **2.** for the oxazolidine substrate shown in the Schemes. Note that in this substrate, boron trifluoride (BF_3) is the Lewis acid that catalyzes the reaction; this acid has been proven to be effective in producing high yields when used in small amounts (12). The protecting group bonded to the nitrogen center is tosyl (Tos). This substituent is electron withdrawing, and there is some evidence that it can improve stereoselectivity (13). A long-term goal of this project is to model the reaction profiles for the substrate where R=H (secondary carbinol carbon), and R=Me (tertiary carbinol carbon). Past results suggest that the latter exhibits improved stereoselectivity (13).

RESULTS AND DISCUSSION

Using quantum mechanical electronic structure methods, I have optimized the structures of the four oxazolidine enantiomers, the eight iminium cation stereoisomers, and the four pyrrolidine

products (cf. **Scheme 1.**). Their total and relative energies are shown in Tables **1. and 2.** It is clear from these data that the conversion from oxazolidine to pyrrolidine is highly exergonic, while the iminium cation intermediates are considerably destabilized with respect to the oxazolidine starting material. The latter is probably due to the tosylate protecting group, which draws electron density from the open ring and destabilizes it.

The high energy of the iminium cation intermediates suggests that the activation barriers for the oxazolidine opening step are probably quite large. I have located two of the four transition states for this step, and they are shown in **Tables 3.** and **4.** The calculated activation energies are 17.4 kcal/mol, for the *trans beta* oxazolidine opening to the *alpha boat up* iminium cation, and 21.9 kcal/mol**,** for the *cis alpha* oxazolidine opening to the *alpha boat down* iminium cation. Note that each one of the four oxazolidine stereoisomers opens to one iminium cation conformation, as indicated in **Tables 3.** and **4.** This has been confirmed by GSM calculations (see Details of the Calculations, below).

Oxazolidine	Iminium Cation	Pyrrolidine
trans beta -1700.57635251	alpha *boat* ***up*** -1700.552102 alpha *chair* ***up*** -1700.566085	*trans* alpha -1700.61448269
cis beta -1700.57875859	alpha *chair* ***down*** -1700.550649 alpha *boat* ***down*** -1700.560290	*cis* alpha -1700.6074275
trans alpha -1700.5840558	beta *boat* ***down*** -1700.553487 beta *chair* ***up*** -1700.559708	*cis* beta -1700.61007708
cis alpha -1700.586516	beta *chair* ***down*** -1700.560351 beta *boat* ***up*** -1700.563305	*trans* beta -1700.61016818

Table 1. Total energy values for all structures in Scheme 1. All energies are in hartrees.

Oxazolidine	Iminium Cation	Pyrrolidine
trans beta 23.93	alpha *boat* ***up*** 39.15 alpha *chair* ***up*** 30.37	*trans* alpha 0.00
cis beta 22.42	alpha *chair* ***down*** 40.06	*cis* alpha 4.43
	alpha *boat* ***down*** 34.01	
trans alpha 19.10	beta *boat* ***down*** 38.28 beta *chair* ***up*** 34.38	*cis* beta 2.76
cis alpha 17.55	beta *chair* ***down*** 33.97	*trans* beta 2.71
	beta *boat* ***up*** 32.12	

Table 2. Relative energy values for all structures in Scheme 1. All energies are in kcal/mol.

Oxazolidine	TS	Iminium Cation
trans beta -1700.57635251	-1700.54869	alpha *boat* ***up*** -1700.552102
cis beta -1700.57875859	-	beta *chair* ***up*** -1700.559708
trans alpha -1700.5840558	-	beta *chair* ***down*** -1700.560351
cis alpha -1700.586516	-1700.55171	alpha *boat* ***down*** -1700.56029

Table 3. Total energies for relevant structures in the oxazolidine opening step. All values are in hartrees.

Oxazolidine	TS	Iminium Cation
trans beta 23.93	41.29	alpha *boat* ***up*** 39.15
cis beta 22.42	-	beta *chair* ***up*** 34.38
trans alpha 19.10	-	beta *chair* ***down*** 33.97
cis alpha 17.55	39.40	alpha *boat* ***down*** 34.01

Table 4. Relative energies for structures in the oxazolidine opening step. All values are in kcal/mol.

I have also located two transition state structures for the aza-Cope – Mannich step of the reaction, shown in **Tables 5.-8.** Previous work from our group suggests that, when the oxazolidine substrate has an electron withdrawing substituent at the nitrogen center, the tandem aza-Cope – Mannich reaction occurs in one step. This is indeed the case for the oxazolidine under consideration here, as I failed to locate any stable intermediates after the rearrangement step. Further results from our group established that, for oxazolidine substrates with electron donating substituents at the nitrogen center, the aza-Cope rearrangement is rate determining (i.e., it has the highest activation barriers). Based on the data in **Tables 5.-8.**, the activation barriers for this step range from 8.2 kcal/mol, for the conversion from the *beta chair down* iminium cation to the *trans beta* pyrrolidine, to 18.0 kcal/mol, for the conversion from the *alpha boat down* iminium cation to the *cis alpha* pyrrolidine. When compared to the activation barriers described above, it appears that the oxazolidine-opening step may be rate determining for at least some of the pathways.

Iminium Cation	ACTS	Pyrrolidine
alpha *boat* ***up*** -1700.552102	-	*trans* alpha -1700.61448269
alpha *chair* ***up*** -1700.566085	-	
alpha *chair* ***down*** -1700.550649	-	*cis* alpha -1700.6074275
alpha *boat* ***down*** -1700.560290	-1700.53166	

Table 5. Total energies for relevant structures in the aza-Cope - Mannich step leading to the alpha pyrrolidine product. All values are in hartrees.

Iminium Cation	ACTS	Pyrrolidine
alpha *boat* ***up*** 39.15	-	*trans* alpha 0.00
alpha *chair* ***up*** 30.37	-	
alpha *chair* ***down*** 40.06	-	*cis* alpha 4.43
alpha *boat* ***down*** 34.01	51.98	

Table 6. Relative energies for relevant structures in the aza-Cope - Mannich step leading to the alpha pyrrolidine product. All values are in kcal/mol.

Iminium Cation	ACTS	Pyrrolidine
beta *boat* ***down*** -1700.553487	-	*cis* beta -1700.61007708
beta *chair* ***up*** -1700.559708	-	
beta *chair* ***down*** -1700.560351	-1700.54724	*trans* beta -1700.61016818
beta *boat* ***up*** -1700.563305	-1700.54457	

Table 7. Total energies for relevant structures in the aza-Cope - Mannich step leading to the beta pyrrolidine product. All values are in hartrees.

Iminium Cation	ACTS	Pyrrolidine	
beta *boat* ***down*** 38.28	-	*cis* beta	2.76
beta *chair* ***up*** 34.38	-		
beta *chair* ***down*** 33.97	42.20	*trans* beta	2.71
beta *boat* ***up*** 32.12	43.88		

Table 8. Relative energies for relevant structures in the aza-Cope - Mannich step leading to the beta pyrrolidine product. All values are in kcal/mol.

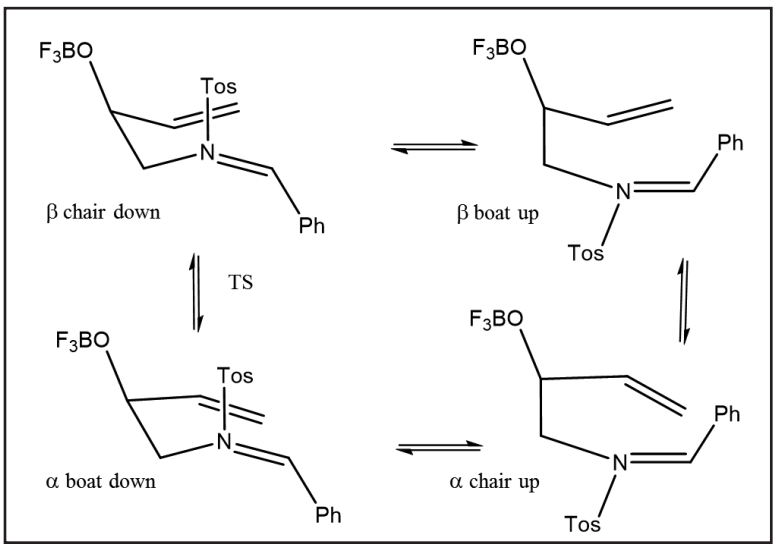

Scheme 3.

As explained in the Introduction, an additional set of pathways that needs to be considered is the series of C-C bond rotations illustrated in **Scheme 2.** There are actually two sets of pathways, each with a different orientation of the phenyl substituent. These are shown in **Schemes 3.** and **4.** There are three, single C-C bonds in the iminium cation structure that can freely rotate (these are shown as single lines in the Schemes). As a result of these rotations, the iminium cation stereoisomers can interconvert.

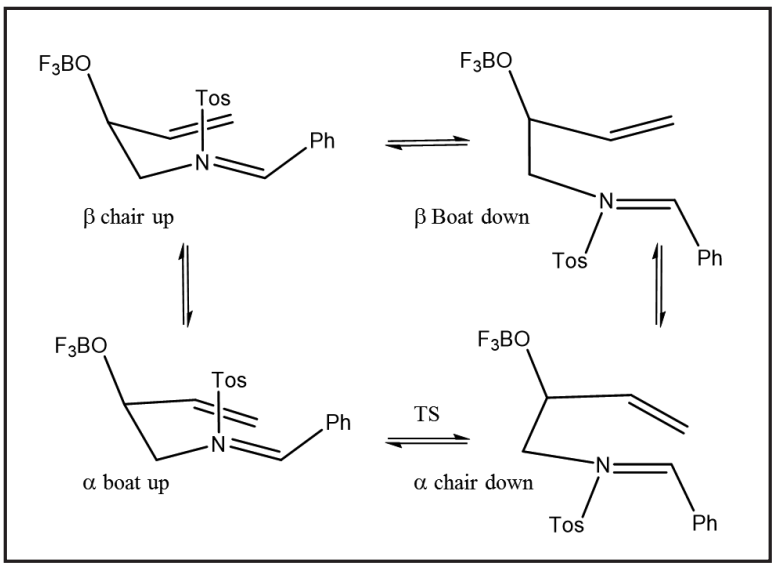

Scheme 4.

The optimized structures of the iminium cations in these pathways are shown in **Figures 4.** and **5.**

Figure 4. Three-dimensional optimized structures of the iminium cations in **Scheme 3.** interconverting as a result of C-C bond rotations. Hydrogen atoms are omitted for clarity. The relative energies of iminium cations and transition states (TS) are shown in kcal/mol.

Figure 5. Three-dimensional optimized structures of the iminium cations in **Scheme 4.** interconverting as a result of C-C bond rotations. Hydrogen atoms are omitted for clarity. The relative energies of iminium cations and transition states (TS) are shown in kcal/mol.

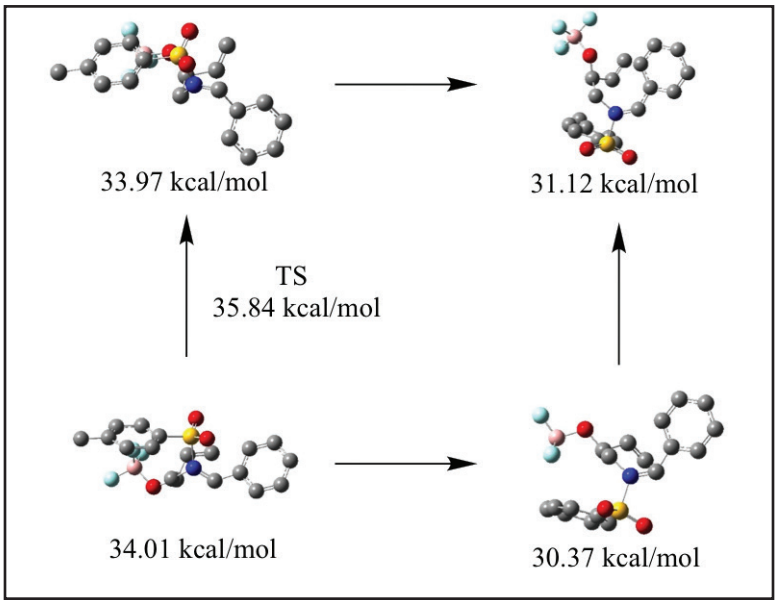

Figure 4.

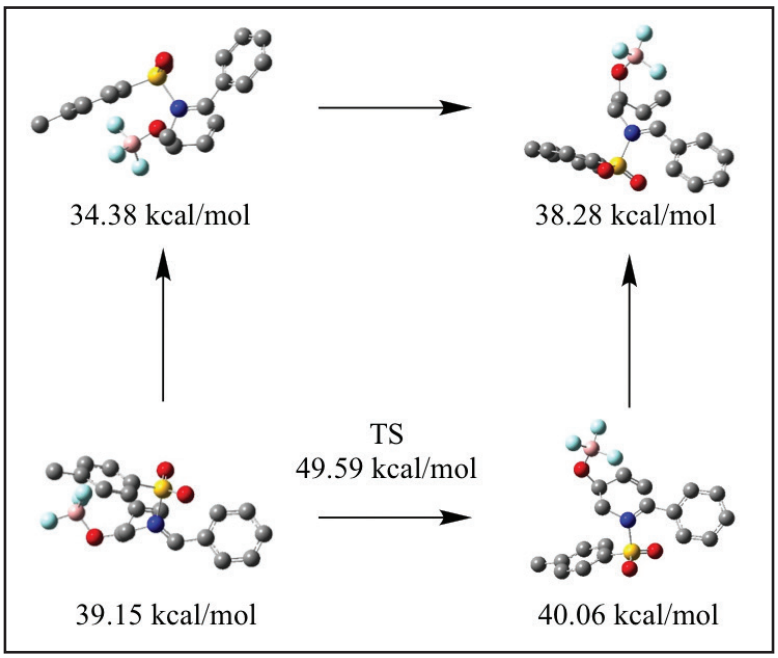

Figure 5.

Figures 4. and **5.** also indicate the relative energies of the iminium cations that are interconverting, and the energies of the two transition state structures that I have located so far. Based on the data shown in the figures, activation barriers can be calculated for two of the rotations: 10.4 kcal/mol, for the interconversion between the *alpha boat up* and the *alpha chair down* iminium cations, and 1.8 kcal/mol, for the interconversion between the *alpha boat down* and the *beta chair down* iminium cations. These values are considerably lower than the barriers for the other steps discussed above, and therefore these pathways are not expected to influence stereoselectivity.

In summary, I have presented preliminary data on the computational analysis of a multistep reaction leading to the formation of a substituted pyrrolidine. The data obtained so far suggest that the initial oxazolidine-step may be rate-determining. Since stereochemistry is not set in this step, the reaction is not likely to occur stereoselectively. However, a complete data set is required in order to make a final determination.

DETAILS OF THE CALCULATIONS

The Gaussian 09 suite of programs was used for all calculations (14). Structures were optimized to a minimum (for the intermediates) or a saddle point (for the transition states), using the Berny algorithm (15). Resulting force constants were used to calculate vibrational frequencies to confirm minima and saddle points. Intrinsic reaction coordinate (IRC) calculations were performed to verify that transition states are on the correct reaction pathway (16). Some of the transition state structures were located using the Growing String Method (17). All calculations were carried out using the M062X density functional (18). Gas phase geometry optimization calculations at the M062X/6-311G(d,p) (19) level of theory were followed by single point calculations using the cc-pVQZ basis set (20). Energy calculations were performed in solvent (dichloromethane) using the IEFPCM polarizable continuum model (21).

REFERENCES

1. (a) Deng, W. and Overman, L.E. *J. Am. Chem. Soc.* **1994**, *116*, 11241-11250. (b) Rizk, A.M. *Naturally Occuring Pyrrolizidine Alkaloids*. ed; CRC Press: Florida, **1991**. pp 2.
2. *Phytochemicals: the Good, the Bad, and the Ugly?* Molyneux, R. J.; Lee, S. T.; Gardner, D. R.; Panter, I. E.; James, L.F. *Phytochemistry* **2007**, *68*, 2973-2985.
3. *Synthesis and Pharmacological Screening of some n-substituted pyrrolidine-2, 5-dione derivatives as potential antidepressant agents*, Bhalgat, C. M.: Darda, P. V.; Bothara, K. G.; Bhandari, S. V.; Ganhdi, J.; Ramesh, B. *Eur. J. Med. Chem.* **2014**, *76*, 508-588.
4. *Synthesis & Evaluation of Antitubercular Activity of Novel Mannich Bases of imidazo[2,1-b][1,3,4]thiadiazoles,* Badiger, N. P. **,** *Adv. Mat. Res.,* **2013,** *1197,* 816-817.
5. (a) *3-Pyrrolidinecarboxylic Acid for Direct Catalytic Asymmetric* anti-*Mannich-Type Reactions of Unmodified Ketones* Zhang, H.; Mifsud, M.; Tanaka, F.; Barbas, C. F. *J. Am. Chem. Soc*. **2006**, *128*, 9630-9631 (b) *Direct Asymmetric* anti-*Mannich-Type Reactions Catalyzed by a Designed Amino Acid* Mitsumori, S.; Zhang, H.; Cheong, P. H. -Y.; Houk, K. N.; Tanaka, F.; Barbas, C. F. *J. Am. Chem. Soc*. **2006**, *128*, 1040-1041; (c) *Catalysis of 3-Pyrrolidinecarboxylic Acid and Related Pyrrolidine Derivatives in Enantioselective* anti-*Mannich-Type Reactions: Importance of the 3-Acid Group on Pyrrolidine for Stereocontrol* Zhang, H.; Mitsumori, S.; Utsumi, N.; Imai, M.; Garcia-Delgado, N.; Mifsud, M.; Albertshofer, K.; Cheong, P. H. -Y.; Houk, K. N.; Tanaka, F.; Barbas C. F. *J. Am. Chem. Soc*. **2008**, *130*, 875-886.
6. *(a) New Strategies in Organic Catalysis: The First Enantioselective Organocatalytic Friedel-Crafts Alkylation Paras, N. A.; MacMillan, D. W. C. J. Am. Chem. Soc.* ***2001****, 123, 4370-4371; (b) Enantioselective Organocatalytic Indole Alkylations. Design of a New and Highly Effective Chiral Amine for Iminium Catalysis Austin,* J. F.; MacMillan*, D. W. C. J. Am. Chem. Soc.* ***2002****, 124, 1172-1173.*
7. *Catalytic Asymmetric Reductive Michael Cyclization* Yang, J. W.; Fonseca, M. T. H.; List, B. *J. Am. Chem. Soc*. **2005**, *127*, 15036-15037.
8. *Carbon-Carbon Bond Formation via Directed 2-Azonia-[3,3]-Sigmatropic Rearrangements. A New Pyrrolidine Synthesis,* Overman, L. E.; Kakimoto*,* M.-A. *J. Am. Chem. Soc.* **1979**, *101*, 1310-1312.
9. For reviews of the aza-Cope rearrangement—Mannich cyclization and related reactions, see (a) The Intramolecular Mannich and Related Reactions Overman, *Comprehensive Organic Synthesis*, L.; Ricca, D. Trost, B. M., Ed.; Pergamon: New York, 1991; Vol. 8, pp 1007-1046; (b) *Charge as a Key Component in Reaction Design. The Invention of Cationic Cyclization Reactions of Importance in Synthesis* Overman, L. *Acc. Chem. Res*. **1992**, *25*, 352-359; (c) *New Reactions for Forming Heterocycles and Their Use in Natural Products Synthesis* Overman, L. E. *Aldrichimica Acta* **1995**, *28*, 107-120; (d) *Chiral Heterocycles by Iminium Ion Cyclization* Bonin, M.; Micouin, L. *Chem. Rev*. **2004**, *104*, 2311-2352; (e) *Molecular Rearrangements in the Construction of Complex Molecules* Overman, L. E. *Tetrahedron* **2009**, *65*, 6432–6446.
10. (a) *Stereoselective Total Synthesis of (±)-Perhydrogenphyrotoxin. Synthetic Applications of Directed 2-Azonia-[3,3]-Sigmatropic Rearrangements* Fukaya, C.; Overman, L. E. *J. Am. Chem. Soc*. **1980**, *102*, 1454-1456; (b) *Synthesis Applications of Aza-Cope Rearrangements. Stereocontrolled Synthesis of Cyclohepta[b]*

pyrrolidines Overman, L. E.; Jacobsen, E. J. *Tet. Lett*. **1982**, *23*, 2737-2740; (c) *Synthesis Applications of Cationic Aza-Cope Rearrangements. Stereoselective Synthesis of* cis- *and* trans-*3a-Aryl-4-oxodecahydrocyclohepta[*b*]pyrroles.* Overman, L. E.; Jacobsen, E. J.; Doedens, R. J. *J. Org. Chem.* **1983**, *48*, 3393-3400; (d) *Carbon-Carbon Bond Formation under Mild Conditions via Tandem Cationic Aza-Cope Rearrangement-Mannich Reactions. A Convenient Synthesis of Polysubstituted Pyrrolidines* Overman, L. E.; Kakimoto, M.-A.; Okazaki, M. E.; Meier, G. P. *J. Am. Chem. Soc*. **1983**, *105*, 6622-6629; (e) *Scope and Mechanism of Tandem Cationic Aza-Cope Rearrangement--Mannich Cyclization Reactions* Jacobson, J.; Levin, J.; Overman L. *J. Am. Chem. Soc*. **1988***, 110,* 4329-4336; (f) *Transition-State Geometry of [3,3]-Sigmatropic Rearrangements of Iminium Ions* Doedens, R.; Meier, G.; Overman, L. *J. Org. Chem*. **1988**, *53*, 685-690; (g) *Enantioselective Total Synthesis of Either Enantiomer of the Antifungal Antibiotic Preussin (L-657,398) from (*S*)-Phenylalanine* Deng, W.; Overman, L. E. *J. Am. Chem. Soc.* **1994**, *116*, 11241-11250; (h) *Controlling Stereoselection in Aza-Cope-Mannich Reactions* Overman, L.; Trenkle, W. *Isr. J. Chem.* **1997***, 37*, 23-30.

11. For recent applications of the aza-Cope rearrangement—Mannich cyclization, see *(a) Asymmetric Total Syntheses of (-)- and (+)-Strychnine and the Wieland—Gumlich Aldehyde Knight, S. D.; Overman, L. E.; Pairaudeau G. J. Am. Chem. Soc.* ***1995****, 117, 5776-5788; (b) Total Synthesis of (±)-Didehydrostemofoline (Asparagamine A) and (±)-Isodidehydrostemofoline Brueggemann, M.; McDonald, A. I.; Overman, L. E.; Rosen, M. D.; Schwink, L.; Scott, J. P. J. Am. Chem. Soc.* ***2003****, 125, 15284-15285. (c) Aza-Cope Rearrangement—Mannich Cyclizations for the Formation of Complex Tricyclic Amines: Stereocontrolled Total Synthesis of (±)-Gelsemine Earley, W. G.; Jacobsen, J. E.; Madlin, A.; Meier, G. P.; O'Donnell, C. J.; Oh, T.; Old, D. W.; Overman, L. E.; Sharp, M. J. J. Am. Chem. Soc.* ***2005****, 127, 18046-18053; (d) A Formal Total Synthesis of (-)-FR901483, Using a Tandem Cationic Aza-Cope Rearrangement/Mannich Cyclization Approach Brummond, K. M.; Hong, S.-P. J. Org. Chem.* ***2005****, 70, 907-916; (e) Total Synthesis of (±)-Actinophyllic Acid Martin, C. L.; Overman, L. E.; Rohde, J. M. J. Am. Chem. Soc.* ***2008****, 130, 7568-7569.*

12. Pendleton, I. and Lindsay, H.A., unpublished data.

13. (a) *Iron(III)-Promoted Aza-Prins-Cyclization: Direct Synthesis of Six-Membered AzacyclesI* R.M. Carballo, M.A. Ramirez, M.L. Rodriguez, V.S. Martin, J.I. Padron *Org. Lett.* **2006,** 8, 3837-3840; (b) *Broadening the Synthetic Scope of the Iron(III)-Catalyzed Aza-Prins Cyclization* R.M. Carballo, G. Valdomir, M. Purino, V.S. Martin, J.I. Padron *Eur. J. Org. Chem.* **2010,** 2304-2313; (c) *aza-Prins-pinacol Approach to 7-Azabicyclo[2.2.1]heptanes and Ring Expansion to [3.2.1]Tropanes* A. Armstrong and S.E. Shanahan *Org. Lett.* (2005) 7, 1335-1338; (d) *aza-Prins-pinacol Approach to 7-Azabicyclo[2.2.1]heptanes: Syntheses of (±)-Epibatidine and (±)-Epiboxidine* A. Armstrong, Y. Bhonoah and S.E. Shanahan *J. Org. Chem.* **2007**, 72, 8019-8024.

14. Gaussian 09, Revision C.01, Frisch, M. J.; Trucks, G. W.; Schlegel, H. B.; Scuseria, G. E.; Robb, M. A.; Cheeseman, J. R.; Scalmani, G.; Barone, V.; Mennucci, B.; Petersson, G. A.; Nakatsuji, H.; Caricato, M.; Li, X.; Hratchian, H. P.; Izmaylov, A. F.; Bloino, J.; Zheng, G.; Sonnenberg, J. L.; Hada, M.; Ehara, M.; Toyota, K.; Fukuda, R.; Hasegawa, J.; Ishida, M.; Nakajima, T.; Honda, Y.; Kitao, O.; Nakai, H.; Vreven, T.; Montgomery, Jr., J. A.; Peralta, J. E.; Ogliaro, F.; Bearpark, M.; Heyd, J. J.; Brothers, E.; Kudin, K. N.; Staroverov, V. N.; Kobayashi, R.; Normand, J.; Raghavachari, K.; Rendell, A.; Burant, J. C.; Iyengar, S. S.; Tomasi, J.; Cossi, M.; Rega, N.; Millam, N. J.; Klene, M.; Knox, J. E.; Cross, J. B.; Bakken, V.; Adamo,

C.; Jaramillo, J.; Gomperts, R.; Stratmann, R. E.; Yazyev, O.; Austin, A. J.; Cammi, R.; Pomelli, C.; Ochterski, J. W.; Martin, R. L.; Morokuma, K.; Zakrzewski, V. G.; Voth, G. A.; Salvador, P.; Dannenberg, J. J.; Dapprich, S.; Daniels, A. D.; Farkas, Ö.; Foresman, J. B.; Ortiz, J. V.; Cioslowski, J.; Fox, D. J. Gaussian, Inc., Wallingford CT, 2009.

15. a) C. Peng, P. Y. Ayala, H. B. Schlegel, and M. J. Frisch, J. Comp. Chem. 17, 49 (1996); b) A. E. Reed and F. Weinhold, *J. Chem. Phys*. **1983**, *78***,** 4066.

16. a) "*The path of chemical-reactions - The IRC approach,*" *Acc. Chem. Res.*,K. Fukui. **14** (1981) 363-68; b). *Theory and Applications of Computational Chemistry: The First 40 Years*, H. P. Hratchian and H. B. Schlegel, Ed. C. E. Dykstra, G. Frenking, K. S. Kim, and G. Scuseria (Elsevier, Amsterdam, **2005**) 195-249.

17. P. Zimmerman*, J. Chem. Theory Comput.* **2013***, 9,* 3043-50.

18. *The M06 suite of density functionals for main group thermochemistry, thermochemical kinetics, noncovalent interactions, excited states, and transition elements: two new functionals and systematic testing of four M06-class functionals and 12 other functionals,* Y. Zhao and D. G. Truhlar. *Theor. Chem. Acc.*, 120 **2008,** 215-41.

19. *Contracted Gaussian-basis sets for molecular calculations. 1. 2nd row atoms, Z=11-18,* A. D. McLean and G. S. Chandler. *J. Chem. Phys.*, 72 (**1980**) 5639-48.

20. *Gaussian-basis sets for use in correlated molecular calculations. 3. The atoms aluminum through argon*, D. E. Woon and T. H. Dunning Jr**.** *J. Chem. Phys.*, 98 (**1993**) 1358-71.

21. a) *Electrostatic Interaction of a Solute with a Continuum. A Direct Utilization of Ab Initio Molecular Potentials for the Prevision of Solvent Effects* Miertuš, S.; Scrocco, E.; Tomasi, J. *Chem. Phys.***1981,** *55*, 117-29; b)*Approximate Evaluations of the Electrostatic Free Energy and Internal Energy Changes in Solution Processes* Miertuš, S.; Tomasi, J. *J.Chem. Phys.***1982,** *65,* 239-45 c) *GEPOL: An Improved Description of Molecular-surfaces. 3. A New Algorithm for the Computation of a Solvent-excluding Surface* Pascual-Ahuir, J. L.; Silla, E.; Tuñón, I. *J. Comp. Chem.***1994,** *15,* 1127-38; d) *A New Definition of Cavities for the Computation of Solvation Free Energies by the Polarizable Continuum Model* Barone, V.; Cossi, M.; Tomasi, J. *J. Chem. Phys.***1997,** *107,* 3210-21; e) *Quantum Calculation of Molecular Energies and Energy Gradients in Solution by Conductor Solvent Model* Barone, V.; Cossi, M. *J. Phys. Chem. A***1998,** *102*, 1995-2001; f) *Geometry Optimization of Molecular Structures in Solution by the Polarizable Continuum Model* Barone, V.; Cossi, M.; Tomasi, J. *J. Comp. Chem.***1998,** *19*, 404-17; g) *Solvent Effect on Vertical Electronic Transitions by the Polarizable Continuum Model,* Cossi, M.; Barone, V. *J. Chem. Phys.***2000,** *112*, 2427-35; h) *Time-dependent Density Functional Theory for Molecules in Liquid Solutions* Cossi, M.; Barone, V. *J. Chem. Phys.***2001,** *115,* 4708-17; i) *Polarizable Dielectric Model of Solvation with Inclusion of Charge Penetration Effects*Cossi, M.; Rega, N.; Scalmani, G.; Barone, V. *J. Chem. Phys.***2001,** *114,* 5691-701; j) *New Developments in the Polarizable Continuum Model for Quantum Mechanical and Classical Calculations on Molecules in Solution* Cossi, M.; Scalmani, G.; Rega, N.; Barone, V. *J. Chem. Phys.***2002,** *117*, 43-54; k) *Energies, Structures, and Electronic Properties of Molecules in Solution with the C-PCM Solvation Model* Cossi, M.; Rega, N.; Scalmani, G.; Barone, V. *J. Comp. Chem.***2003,** *24*, 669-81; g) T. H. Dunning Jr., "Gaussian basis sets for use in correlated molecular calculations. I. The atoms boron through neon and hydrogen," *J. Chem. Phys.*, **90** (1989) 1007-23.